JOURNAL OF MATERIALS SCIENCE 19 (1984) 3588–3592

Subsurface deformation in dry sliding of hypo-eutectic Al–Si alloys

B. N. PRAMILA BAI, S. K. BISWAS
Department of Mechanical Engineering, Indian Institute of Science, Bangalore-560012, India

The subsurface deformation during dry sliding of Al–Si alloys is studied by fragmentation of silicon particles. The size of the fragmented particles does not vary with load. The depth of deformation is found to increase with increase in normal load. This experimental observation agrees with load–deformation depth characteristics obtained by a slip line field model.

1. Introduction

It is known that in dry sliding subsurface deformation plays an important role in controlling wear behaviour [1–13]. In single phase materials the near surface region contains grains elongated in the sliding direction [2]. In a two-phase material such as Al–Si, the deformation of the matrix of α-aluminium causes fragmentation of silicon resulting in a matrix containing finely dispersed particles.

There have been efforts to assess the flow stress at the worn surface by measuring the strain accumulated in the subsurface. Microhardness measurements is a popular method [7, 9], while electron channelling has also been used [11]. Suh [12] has observed that the direction of plastic flow under a static indenter and that during wear are not the same. Hence one may not get a correct description of subsurface deformation by microhardness measurements. In the case of two phase materials with a fine dispersion of second phase particles it is difficult to make a measurable indentation without striking a second phase particle. This can give rise to anomalously high hardness values.

The present work is aimed at studying the effect of silicon content and bearing pressure on subsurface deformation of Al–Si alloys. The parameters that have been studied are the depth of the deformed zone and variation of silicon particle size within the zone. A slip line field model has been proposed for the wear process.

2. Test materials

Composition of the three test (unmodified binary Al–Si) alloys is given in Table I. The microstructure of these alloys consists of dendrites of α-aluminium with silicon segregated in the interdendritic region. It was observed that there is some variation both in the size of the dendritic cells as well as silicon particles. The former has been neglected and the latter has been taken into account in the subsurface studies, as will be discussed later.

3. Experimental methods

A pin on disk machine was used for conducting wear experiments. Cylinders (pin) of diameter 10 mm and length 11 mm were machined from cast fingers of test alloys. Wear was measured as the weight lost. Two sets of wear tests were carried out by sliding the pin against hardened (55 RC) EN24 disks under the following conditions:

(i) Specimens at different silicon content were worn at a load of 19.6 N (0.26 MPa) at a speed of 5.2 m sec^{-1} over a sliding distance of 6.5 km.

(ii) For 8% Si alloy, experiments were conduc-

TABLE I

Alloy No.	% Si
1	2.04
2	4.06
3	5.81
4	8.02
5	12.32

0022–2461/84 $03.00 + .12

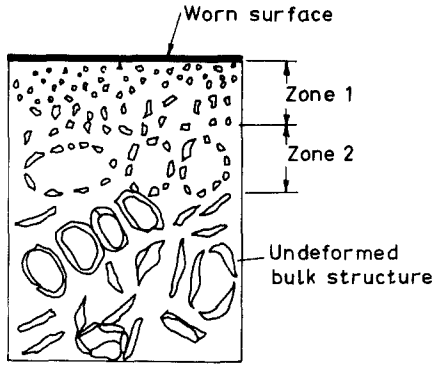

Figure 1 Schematic diagram of subsurface structures. Different zones are marked.

ted at loads of 4.9 N, 9.8 N, 19.6 N, 29.4 N and 39.2 N. Sliding speed (5.2 m sec^{-1}) and sliding distance (6.5 km) were kept constant.

The surface studies were done on oblique sections which intersected the worn surface along a diametral line parallel to the wear tracks at an angle of 6°. The sectioned surface was polished with diamond paste and etched with 0.5% HF. The appearance of the subsurface is shown schematically in Fig. 1. The region adjacent to the wear track, characterized by randomly dispersed silicon particles, is referred to as Zone 1. Zone 2 contains fragmented silicon which is still retained in interdendritic locations.

4. Results

As no particular trend was observed in the depth of Zone 1 across the diameter of the specimen, an average of depth was obtained and shown as a function of silicon content and load in Figs. 2 and 3 respectively. Since the size of silicon in the

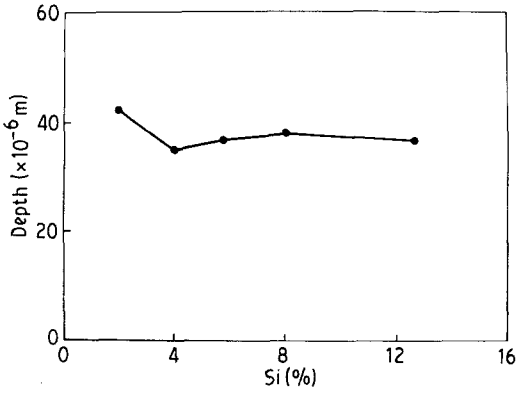

Figure 2 Variation of average depth of Zone 1 with silicon content.

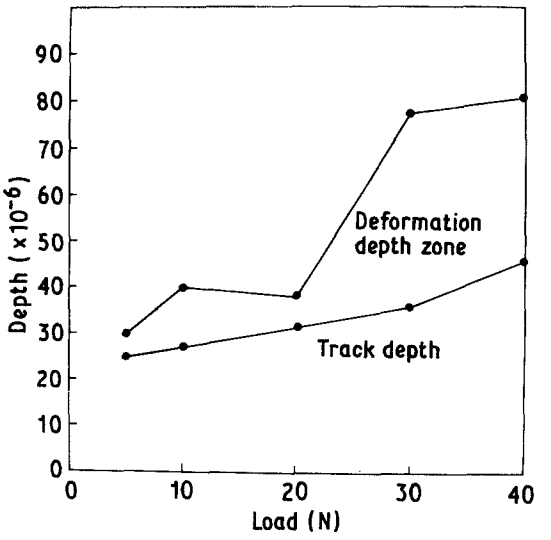

Figure 3 Variation of average depth of Zone 1 with normal load. Corresponding track depths are also shown.

undeformed structure is not the same for all cases, the average size measured in the subsurface was normalized with respect to length and breadth of silicon in the undeformed structure. Fig. 4 shows such normalized size plotted against distance from worn surface, at different loads. Load does not seem to have any significant influence on the particle size–depth characteristics. Fig. 5 shows the variation of microhardness with distance from the worn surface. The hardness of matrix is more or less uniform in the deformed region and is greater than that in the undeformed region. The

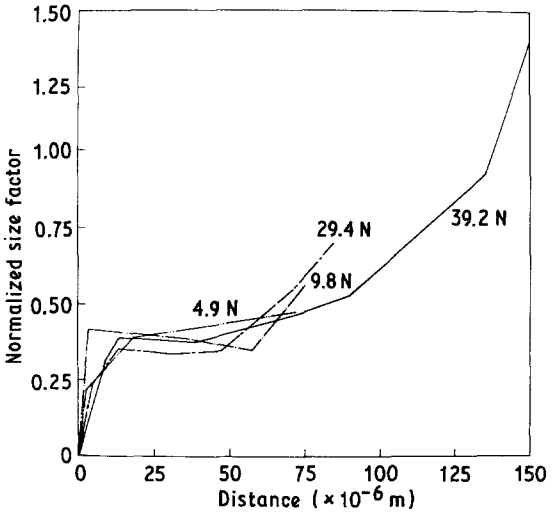

Figure 4 Variation of average particle size with distance from wear tracks at different loads.

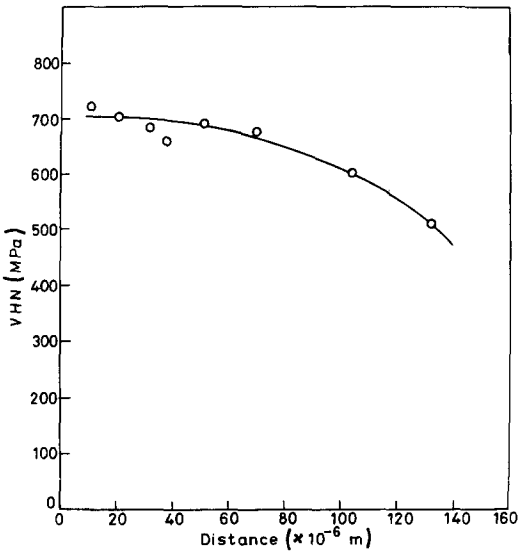

Figure 5 Variation of microhardness with distance from worn surface.

region of uniform hardness approximately corresponds to Zone 1 at that spot.

5. Discussion

The subsurface region of worn Al–Si alloys has been shown to contain fragmented silicon particles. A model for the fragmentation of the particles is shown in Fig. 6. The α-aluminium matrix is able to flow if either the silicon needle is deforming simultaneously with it or if the needle is becoming fragmented. The former seems unlikely to occur in the present case since silicon becomes plastic only above 500° C [14]. The latter can therefore be considered to be the operating mechanism.

It is hypothesized here that the fragmentation is a function of strain that the matrix experiences. For a strain hardening material, the subsurface hardness can be expected to reach a maximum and then decrease with depth. Microhardness measurements on the worn Al–Si specimens do not show this trend (Fig. 5). The particle size variation with depth (Fig. 4) however points to the development of high plastic strains near the surface. The strain decreases rapidly with depth until a stable value is reached at about 13 μm. This trend seems to be independent of normal load.

A slip line field is proposed to model the (plane strain) deformation depth–load behaviour in dry sliding. It is a variation of Rowe's indentation and ploughing model [15] and is shown in Fig. 7a. An asperity (of the hard disk material) has sunk in under normal load. When the asperity slides (pin) material piles up in front. It is assumed that the frontal pile-up accounts for the total volume displaced by the asperity. This fixes the pile-up boundary AZ and a zone of incipient plastic flow bounded by $G_1\ B_1\ C_1\ Z$ and $G_1\ C'A'\ Z$. The coefficient for friction is given by

$$\mu = \frac{\cos 2\gamma}{q/k},$$

where $\gamma = 30°$ in Fig. 7a, q is the normal stress and k is the shear stress. Triangles AC_1B_1 and AA_1Z correspond to rigid material. A 5° network has been used for construction of slip lines. The corresponding hodograph [16] in Fig. 7b shows a horizontal streamline of unit velocity crossing the discontinuity $A'Z$ and eventually emerging with unit velocity in the horizontal direction across discontinuities G_1F', $F'E' \ldots B'C'$.

The hard asperity which is removing material from the soft aluminium–silicon pin is most probably the edge of a deposit on the steel surface. Due to the propensity of aluminium alloys to seize when rubbed against steel, deposits of size (height and breadth) 50 to 100 μm, are formed. Considering that the experimentally observed depth of Zone 1 is also of the order of 50 to 100 μm and that the maximum depth estimated using the slip line field model is of the same order as that of the

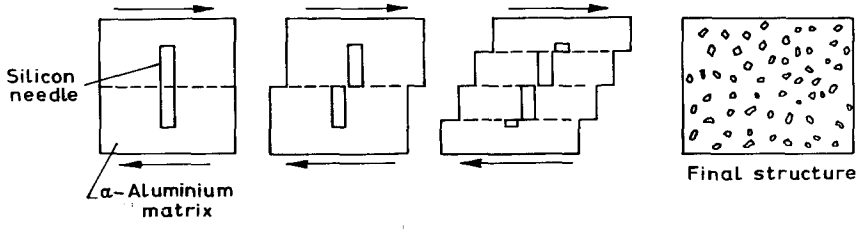

Figure 6 A model for fragmentation process.

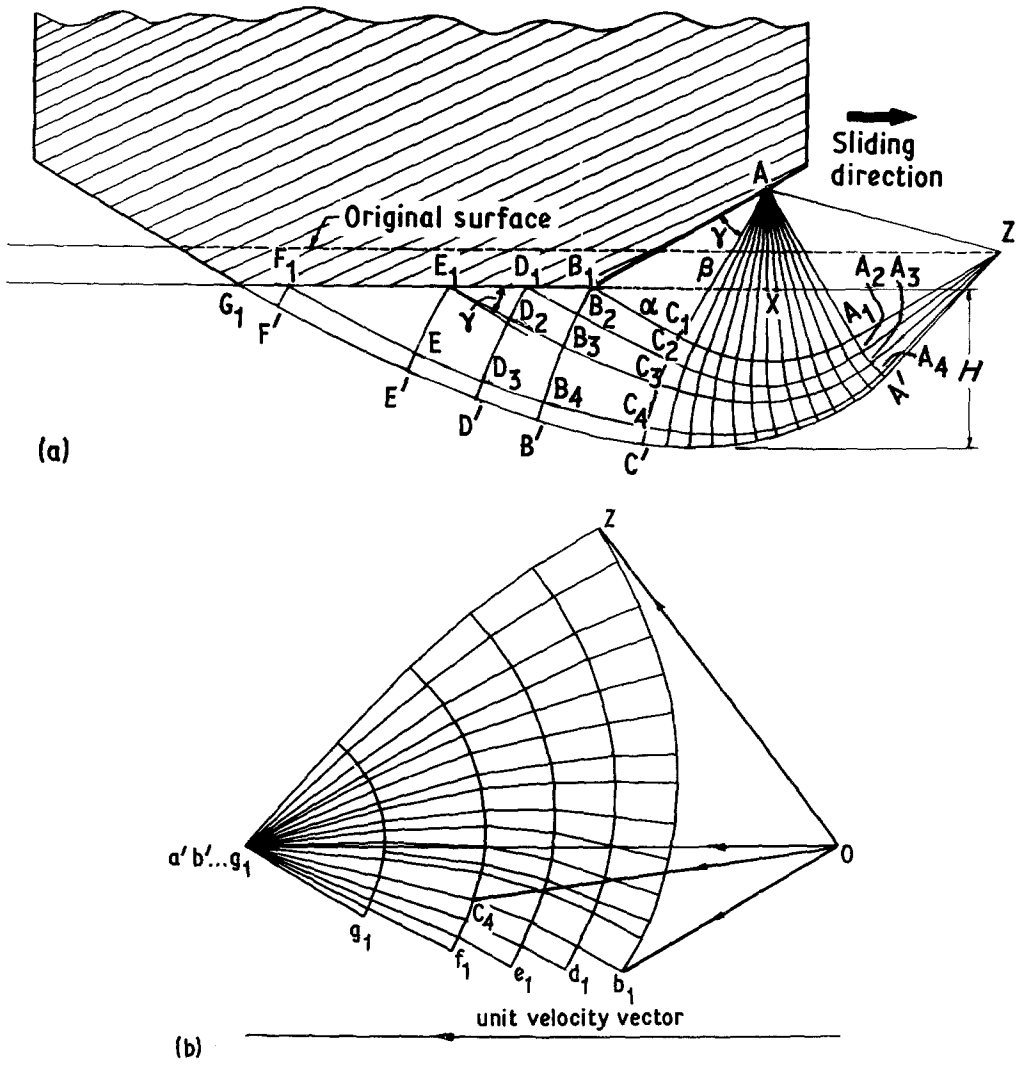

Figure 7 (a) Proposed slip line field. (b) Hodograph for the above. The asperity is considered to be stationary and material is sliding from right to left.

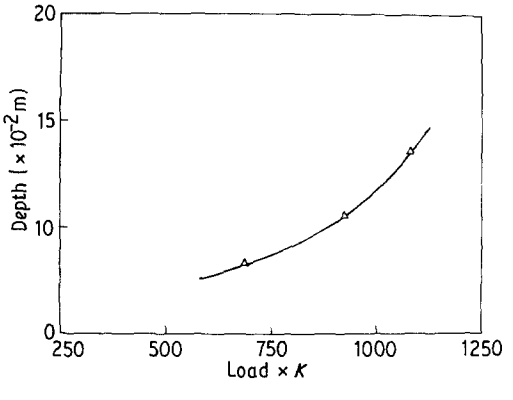

Figure 8 Load–deformation depth characteristics as calculated by the slip line field.

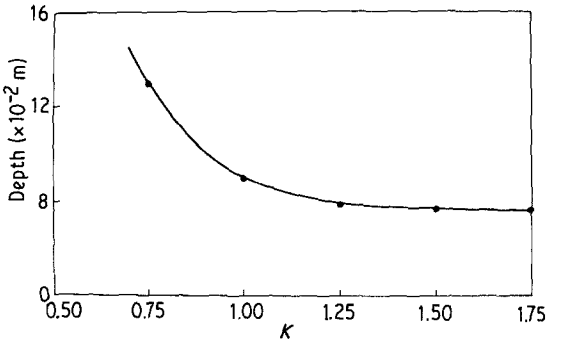

Figure 9 Variation of calculated depth of deformation with strength.

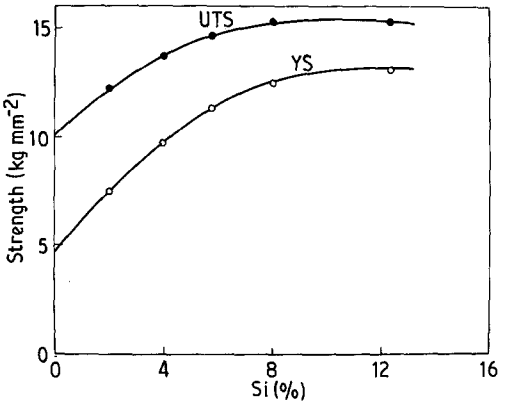

Figure 10 Effect of silicon content on strength.

assumed asperity, the model could be said to be reasonably realistic. Integration of pressure over the contact area of the asperity gives the normal load corresponding to a given "sinking" of the asperity. The deformation depth–load characteristics (Fig. 8) show a trend similar to that observed experimentally (Fig. 3). Now for a given asperity sinking and deformation depth H, if the load is assumed to be a linear function of the material strength K, characteristics such as that shown in Fig. 8 can be obtained for different material strengths (multiples of K). From this a depth–material strength characteristic (at constant load) can be constructed (Fig. 9). As the strength increases the depth falls sharply until the strength is equal to $1K$ beyond which the reduction in depth is gradual. Fig. 10 shows the strength of aluminium alloys to increase with silicon content. Referring to Fig. 2, although the trend between 2 to 4% Si seems to suggest the validity of the above model, the lack of definitive trend in depth as a function of material strength at other silicon percentages seems to indicate that the single asperity model based on strength considerations is not adequate to explain the dry sliding process. Multiple asperity interactions, possible changes in coefficient of friction and adhesion are factors which should possibly be taken into account to make the model more realistic.

6. Conclusions

1. The extent of silicon fragmentation in the subsurface of worn aluminium–silicon alloy is a good qualitative indicator of subsurface strains.
2. Strain in the deformed subsurface does not vary with normal load.
3. Depth of deformation increases with load.

Acknowledgements

This work was carried out under a grant from the Council of Scientific and Industrial Research, Government of India.

References

1. N. P. SUH, *Wear* **25** (1973) 111.
2. D. A. RIGNEY and W. A. GLAESER, *ibid.* **46** (1978) 241.
3. B. N. PRAMILA BAI, E. S. DWARAKADASA and S. K. BISWAS, *ibid.* **71** (1981) 381.
4. R. C. BILL and D. W. WISANDER, *ibid.* **41** (1977) 351.
5. J. A. B. VAN DIJCK, *ibid.* **42** (1977) 109.
6. W. A. GLAESER, *ibid.* **47** (1977) 393.
7. K. L. HSU, T. M. AHN and D. A. RIGNEY, *ibid.* **60** (1980) 13.
8. J. H. DAUTZENBERG, *ibid.* **60** (1980) 401.
9. M. A. MOORE and R. W. DOUTHWAITE, *Met. Trans. Ser. A* **7** (1976) 1833.
10. D. A. RIGNEY and J. P. HIRTH, *Wear* **53** (1979) 345.
11. A. W. RUFF, *ibid.* **40** (1976) 59.
12. N. P. SUH, *ibid.* **44** (1977) 1.
13. A. A. TORRANCE, *ibid.* **50** (1978) 169.
14. W. D. SYLWESTROWICZ, *Phil. Mag.* **7** (1962) 1825.
15. G. W. ROWE and A. G. WETTON, *J. Inst. Metals* **97** (1969) 193.
16. M. S. L. KUBENDRAN and S. K. BISWAS, *Int. J. Mech. Sci.* (submitted).

Received 25 July 1983
and accepted 24 January 1984